Case Studies in Construction Materials 18 (2023) e02142

Contents lists available at ScienceDirect

Case Studies in Construction Materials

journal homepage: www.elsevier.com/locate/cscm

Short communication

Full-scale sustainable structural concrete containing high proportions of by-products and waste

Amaia Santamaría [a], Víctor Revilla-Cuesta [b,*], Marta Skaf [c], Jesús M. Romera [a]

[a] Department of Mechanical Engineering, Escuela de Ingeniería de Bilbao I, University of the Basque Country, Pl. Ingeniero Torres Quevedo 1, 48013 Bilbao, Spain
[b] Department of Civil Engineering, Escuela Politécnica Superior, University of Burgos, c/ Villadiego s/n, 09001 Burgos, Spain
[c] Department of Construction, Escuela Politécnica Superior, University of Burgos, c/ Villadiego s/n, 09001 Burgos, Spain

ARTICLE INFO

Keywords:
Electric arc furnace slag
Ground granulated black furnace slag
Ladle furnace slag
Quarry tailings
Recycled concrete aggregate
Sustainable concrete
Fresh properties
Shrinkage
Water penetration
Chloride penetration

ABSTRACT

The construction industry in general is, through minor low-cost processing methods, converting several of its by-products into viable materials; furthermore, some siderurgic sector by-products are likewise of use. In this context, large-scale batches (mix volumes over 0.5 m^3) of good quality structural concrete are proposed, in which two kinds of binder and two kinds of aggregate (steel slag and recycled concrete) are used to perform four concrete mixtures, containing more than 80 % in mass of good-quality recycled materials. A batch of tests, both in the fresh and in the hardened state, are performed, covering on-site placement and long-term properties, to guarantee the suitability and the quality of the mixtures as structural concretes. Most of the results were encouraging, mainly depending on the aggregate and the binder types that were used. The fresh-state workability of all the test mixtures was good. All the results in terms of hardened properties, strength (42 MPa in type I cement mixtures, and 32–38 MPa in type III cement mixtures), stiffness, long-term shrinkage, and microstructural state (porosity, permeability) were acceptable, their quality depending on the type of each component. The good results of the mixtures based on the slag-based binder deserve attention. Some weak points found were the slightly higher specific weight of the slag aggregate mixes (amounting to more than 2.7 Mg/m^3), plastic shrinkage rates (in some cases greater than 1.2–1.5 thousand), and loss of resistance against chlorine penetration in recycled concrete mixes. However, drawbacks of that sort are no obstacle to their use in most structural applications.

1. Introduction

In the field of civil engineering, the construction and the architecture of buildings are both activities in which the use of hydraulic mixes is a necessary priority [1,2]. Over the past century or so, the main characteristics of concrete mixtures, placement, strength, and durability, have greatly improved. The use of concrete has been globalized, due both to its low-economic cost and its affordability. However, another issue is affecting its widespread usage in the 21st century: sustainability [3]. Hence, the fact that as much as one ton of CO_2 is emitted per ton of concrete that is laid calls for alternatives [4,5].

Concrete is now understood to be a material in which significant amounts of waste and by-products could be included, provided

* Corresponding author.
E-mail address: vrevilla@ubu.es (V. Revilla-Cuesta).

https://doi.org/10.1016/j.cscm.2023.e02142
Received 10 February 2023; Received in revised form 4 May 2023; Accepted 11 May 2023
Available online 12 May 2023

that those materials are of sufficient quality [6]. It has been demonstrated that industrial waste products can be transformed into viable products for inclusion in both Portland cement and concrete [7,8]. Will these additions imply a loss of concrete quality and economic competitiveness? Just how far can the inclusion of waste products be useful for the viability of concrete products? Undoubtedly, the challenge for civil engineers concerns the conservation (or improvement) of concrete performance after by-products have been added. Finally, waste products are also generated within the activity of the construction sector; a further question might therefore be to what extent the sector is capable of recycling its own waste. If we wish to take steps towards sustainability, we are compelled to study such questions.

One of the by-products, "quarry tailings", is a dusty material also known as "limestone fines from milling", produced in abundance when quarrying (LFQ). Its quality is as high as other quarried products and its overly fine particles are is only inconvenience. Often stored in heaps around quarries in the surrounding region, its effective application in mortars and concrete is a priority.

It is also worth mentioning "Construction and Demolition Wastes" (CDW) as a heterogeneous waste product accounting for a third of all waste generated in the EU, mainly from demolition. Initially, this waste is a low-quality, heterogeneous material (with remnants of wood, plastic, plaster, ceramic, and metallic fragments), of little utility. In contrast, a none too dissimilar material, Recycled Concrete Aggregate (RCA), from the crushing and milling of useless concrete structures and defective precast components (from the precast concrete industry) is a higher quality waste than CDW [9], being suitable for the preparation of concrete mixtures [10–12]. Pre-cast components were used to obtain the RCA used in this study [13].

Another sector from which by-products are drawn is the siderurgic industry (siderurgy, from the Greek roots σίδηρος iron and ἔργον work), which has seen its environmental impact increase, mainly since the invention of the Bessemer converter in the mid-19th century, and the consequent extension of the steelmaking industry around the world. Good quality non-metallic steelmaking by-products can be of great utility to the construction sector [14–16].

Among the long list of iron and steelmaking industrial by-products, some are initially discarded (dross, muds, and other metallic waste…), and the others (petrous-mineral wastes) must be re-used, to give added value to concrete. Globally, all forms of slag might be evaluated, although engineering criteria should be applied to their selection/reconversion, as slags are not always suitable for direct inclusion in concrete mixes [17,18].

Ground Granulated Blast Furnace Slag (GGBS), Electric Arc Furnace Slag (EAFS), Ladle Furnace Slag (LFS) and even Converter/BOF slag or cupola furnace and Argon Oxygen Decarburization (AOD) converter slags have all been positively evaluated in previous studies as suitable raw materials for concrete [19], although they must be treated with caution, due to the presence of dangerous substances that can disrupt their volumetric stability [20,21]. The first of them, GGBS, has been successfully used for over a century [22] as an active addition in Portland cement. Its suitability for marine works is widely acknowledged and examples can be found in port seawalls and docks around the world. The second by-product, oxidizing/black EAFS, has been used as coarse and as fine aggregate in hydraulic [23–25] and bituminous concrete [26–28] after weathering and raking for over 20 years with satisfactory results. Finally, basic/white LFS, a dusty fine aggregate in many mortar and concrete applications [29,30], which also serves as a carbon sequestrator, was used in this study.

Our research team has throughout the 21st century committed itself to advancing reliable alternative construction materials [31, 32], converting siderurgic and construction by-products into concrete aggregates [33–35] and efficiently recycling these industrial wastes. The inherent challenges of our work concern the mitigation of environmental impact and the enhancement of global sustainability.

1.1. Research significance

In this study, four concrete mixtures of promising quality, selected on the basis of their relevance, were developed to verify their practical performance. The purpose here was to ensure that the mixtures fulfilled two conditions, among others. The first condition was that the mixes had to consist of at least three fourths by mass of recycled materials; hence, their net emissions will amount to one half of the standard "real concrete" emissions. The second was an engineering condition: half a cubic meter of concrete was prepared in each batch, a lesser part for testing with conventional methods, and the greater part to produce realistic structural components for construction and building engineering.

The idea that laboratory tests on small size mixtures are sufficiently representative to characterize batches of concrete for use in civil works (of several cubic meters) is disregarded in this work. The present methodology is innovative in several ways, in so far as answers are sought to the questions that arise in structural concrete engineering. In this way, the properties of the concrete were verified in a representative way using specifically treated samples, as will be described in the following sections. Both fresh and hardened behaviors have been evaluated, as well as other characteristics: short and long-term shrinkage, porosity/permeability, and chlorine ion penetration. The results of structure and volumetric stability analyses confirmed their suitability for use in robust structural components [36–40].

2. Materials

2.1. Cement, water, admixtures, and natural limestone

Two different types of cement were used in this study: a Portland cement type CEM I 52.5 R, and a Portland cement type CEM III/A 42.5 N; both as specified in standard EN 197–1 [41]. The composition, specific gravity, and Blaine specific surface values of each cement are presented in Table 1. Drinking water that contained no harmful compounds that could affect the quality of the mixes was

taken from the urban mains supply to the University of Burgos.

Two different admixtures, also used in other studies by the same authors [13] ensured a suitable workability; on the one hand, a viscosity regulator to enhance the flowability of the mixtures, and on the other hand, a plasticizer to reduce the water demand.

The fine fraction of a crushed natural limestone (limestone fines quarrying, LFQ, calcite fraction >95 %), with a maximum aggregate size of 0.6 mm (No. 30 sieve) and fineness modulus 1.1 units, was used. Its granulometric curve is shown in Fig. 1 and other characteristics are included in Table 3. It is worth mentioning that the addition of these limestone fines improved mix workability, as some of the authors of this study have shown elsewhere [35], compensating the lack of particles smaller than 0.6 mm in RCA and especially in EAFS aggregate.

2.2. EAFS and LFS physical-chemical properties

Three common size fractions (0–4 mm; 4–12 mm; 12–20 mm) of Electric Arc Furnace slag (EAFS) were used in this research. It was treated before its reuse in the following way: cooling in a pit, primary crushing, magnetic separation of metal oxides, milling to suitable sizes, and finally three-months of outdoor weathering, raking, and turning the heaps every month. The chemical composition of EAFS, obtained by XRF (X-ray fluorescence) is specified in Table 2. The fineness moduli of the three size fractions, 0–4 mm, 4–12 mm, 12–20 mm, were 3.9, 5.7, and 7 units, respectively, and their granulometry is shown in Fig. 1.

The main properties of EAFS aggregate (gravel sizes), in comparison with other natural and artificial aggregates for concrete, are higher density, notable superficial roughness and angularity, high abrasion resistance, good toughness-fragmentation resistance, high strength-stiffness, and chemical basicity [42,43]. Specific data on EAFS properties can be found in a previous study [35] in which some of the authors of the present study were involved; other researchers have found similar results analyzing the properties of this type of slag [44]. The EAFS fractions were pre-soaked with water before the mixing operations, to avoid unexpected short-term losses in the workability, due to their quick absorption of high-levels of water.

LFS is a dusty powdery material whose granulometry is shown in Fig. 1. It has a fineness modulus of 0.7 units, and its chemical composition and specific gravity are respectively specified in Table 2 and Table 3. As with EAFS, supplementary data on this material may be found in previous works of the authors [30].

2.3. RCA and supplementary siliceous sand physical-chemical properties

The RCA consisted of rejected pieces of precast concrete, observed to have geometric and aesthetic defects after demolding in the manufacturing process, that had been crushed at a nearby manufacturing plant; the nominal compressive strength of the original concrete was greater than 45 MPa. After crushing, the concrete was sieved and separated into two fractions (0–4 mm; 4–12.5 mm), whose gradation is also shown in Fig. 1. Its chemical composition is shown in Table 2, and some physical properties are listed in Table 3, such as density and water absorption at 24 h, tested in accordance with EN 1097–6. These RCA aggregates were also pre-soaked for use in concrete mixtures, with the objective of homogenizing the industrial manufacturing of concrete [13].

A local siliceous river sand, washed and free of clay, the size and grading of which were previously presented in Fig. 1, was added to enhance the poor original quality of the RCA aggregate fractions, shown in the last column of Table 3.

3. Dosage and mixing

Four different concrete mixes were designed in the development of this research. They contained either EAFS or RCA in the highest possible proportions as the first variable to enhance the sustainability, and their designs guaranteed the concrete quality for structural applications. They were labelled IS (CEM I cement, EAFS-based aggregate); IRC (CEM I cement, RCA-based aggregate); IIIS (CEM III/A cement, EAFS-based aggregate); and IIIRC (CEM III/A cement, RCA-based aggregate). In general, EAFS or RCA constituted the totality of the coarse aggregate and a high proportion of the fine aggregate; natural/conventional aggregates were revealed as indispensable in the smaller fractions to achieve an ideal grading and a suitable quality of concrete. In the EAFS mixtures [44,45], a mix of small-sized EAFS (0–4 mm, low content of fines, grading in Fig. 1), and the above-mentioned fine fraction (0–0.6 mm) of limestone aggregate (also in Fig. 1) were used as fine aggregate. In the RCA mixtures, both siliceous sand (0–4 mm) and the limestone fines LFQ (0–0.6 mm) were added to complete the fine RCA fraction (0–4 mm).

The two different Portland cement types (CEM I and CEM II/A) used to manufacture the mixes were the second variable to affect their sustainability. CEM I, a basic standard cement type in construction, was used in the IS/IRC mixtures, and a certain proportion (14

Table 1
Chemical composition of cements.

Compounds	CEM I 52.5 R	CEM III/A 42.5 N
Portland Clinker (%)	90	50
Calcium Carbonate (%)	5	-
Calcium sulfate (%)	4.5	2
Ground granulated blast furnace slag (%)	-	47
Density (Mg/m^3)	3.15	3.05
Blaine specific surface (m^2/kg)	450	540

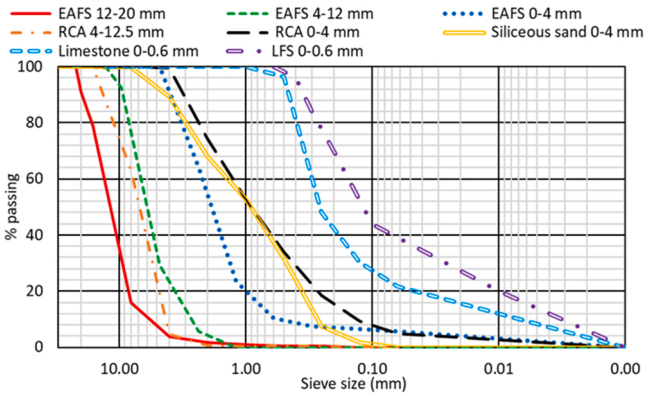

Fig. 1. Granulometric aggregate curves.

Table 2
Chemical composition of EAF/LF slags and RCA by XRF.

Compounds	EAFS	RCA	LFS
Fe_2O_3 (%)	22.3	1.1	1.2
CaO (%)	32.9	20	59.2
Free CaO (%)	0.8	-	8.2
SiO_2 (%)	20.3	50.8	21.3
Al_2O_3 (%)	12.2	3.7	8.3
MgO (%)	3.0	0.6	7.9
MnO (%)	5.1	0.1	0.26
SO_3 (%)	0.42	1	1.39
Cr_2O_3 (%)	2.0	0.1	-
P_2O_5 (%)	0.5	0.06	-
TiO_2 (%)	0.8	0.15	0.17
$Na_2O + K_2O$	0.2	0.8	0.4

Table 3
Physical properties of the aggregates.

Aggregate	Saturated-surface-dry density (Mg/m^3)	Water absorption (%)	Los Angeles loss/Sand friability
EAFS	3.42	2.12	12
LFS	3.03	-	-
Coarse RCA	2.42	6.25	35
Fine RCA	2.37	7.36	16
Siliceous sand	2.58	0.25	9
Limestone fines LFQ	2.65	0.6	-

%) of LFS was added to the CEM I as SCM (Supplementary Cementitious Material) to reduce clinker consumption and to enhance sustainability; some effects of that LFS addition were also indirectly evaluated [46]. The second cement, CEM III/A type, a more sustainable and less costly binder, contains almost 50 % of GGBS, a valuable waste produced in the ironmaking industry, after quenching the molten slag and then grinding it down to a fine powder. A binder proportion of 300 kg/m^3 and an effective w/c ratio of 0.4–0.45 units, frequent values for structural mixtures [47], were applied to obtain a compressive strength close to 40 MPa after 28 days.

Apart from suitable grading, the third variable used in the mix design was fresh workability, the purpose was to obtain two classes of workability: Pumpable (P) and Self-Compacting (SC) mixes. It has an indirect effect on sustainability and is key to successful structural concrete mixes. A high presence of EAFS in concrete mixes is known to lower mix workability, due to the superficial roughness of their particles; additionally, the higher density of the EAFS particles implies a higher tendency toward decantation-segregation when in suspension within a fluid matrix. On the contrary, the RCA showed less density than the conventional aggregates, and the surface roughness of its particles was less aggressive. Therefore, the prudent objectives were to perform pumpable EAFS mixtures and self-compacting RCA mixtures. Initially, the goal was a slump of 200 mm for the pumpable mixes, and the target for the self-compacting mixes was a spread of 600 mm (of which 500 mm in over four seconds), both after the Abram's cone test. The inclusion in the RCA mixtures of a siliceous river sand fraction 0–4 mm, and the presence of LFQ 0–0.6 mm were decisive, in so far as they attenuated the surface roughness effect.

The in-volume final granulometry of the whole aggregates used in the mixes is shown in Fig. 2 and the in-weight proportions are

detailed in Table 4. Before the present experimental campaign was performed, laboratory scale mixes were developed to ascertain the definitive proportions used in this work [35]. The EAFS aggregate fractions, 0–4, 4–12, and 12–20 mm, and the RCA fractions, 0–4 and 4–12.5 mm, were both pre-soaked. According to the data presented in Table 4, the water (w), cement (b), and occluded air (a) within the mixes corresponded to more or less 26 % by volume; in fact, similar volumes of cement were used in all the mixes (around 10 %), the water content was around 12 %, and the occluded air 3–4 %. The volumetric composition of the remaining 74 %, see Fig. 2, were key to obtain a suitable mix workability and enhanced sustainability.

The percentage of EAFS by volume in pumpable mixes (IS and IIIS), regarding the whole mix, reached approximately 50 % (1720 kg), and the limestone fines at 24 % (640 kg). In all, 74 % in volume (as said in the former paragraph) and 2470 kg in weight. The cementitious matrix amounted to approximately 24 %+ 26 % (w/b/air) = 50 % in volume.

In the RCA self-compacting mixes, IRC and IIIRC, the volume of RCA amounted to around 49 % · (24 %+25 %), weighing 1180 kg; after adding volumes of limestone fines (360 kg/13.5 %) and siliceous sand (300 kg/11.5 %), we have 74 % in volume and 1840 kg in weight. The cementitious matrix (≤ 0.6 mm) amounted to 26% (w/b/a) +35 % · (25 % fine RCA) + 30 % · (11.5 % fine sand) + 13.5 % fine limestone= 52 %.

The global in-weight proportion of recycled materials within the pumpable mixes, with respect to total concrete, was 1720 kg of EAFS and 640 kg of quarry waste (limestone fines LFQ) in 2790 kg of concrete, *i.e.*, 84.5 %, and as much as 86 % in the IS mixture with LFS, and 90 % in the IIIS mixture, due to GGBS. Likewise, the recyclable materials in the self-compacting RCA mixes amounted to about 70 % in IRC (1180 RCA+360 limestone + 42 Kg LFS = 1580 kg) in 2260 kg of concrete, and 75 % in IIIRC (1180 RCA+360 limeston+150 GGBS=1690 kg) in the same 2260 kg.

Four concrete mixes of 500 L were successively used in the pouring/filling of a large 35-liter formwork of four beams, considered beyond the scope of this research, and the remaining material was used to manufacture (cubic, cylindrical, small prismatic, large prismatic…) samples for the exhaustive fresh and hard-state material characterizations that are described in this study.

4. Fresh state properties of mixtures

The consistency test results are presented in Table 5. EAFS pumpable concretes achieved an S4 consistency class (slump 160–210 mm). Slight vibration of the formwork was necessary when the large pieces were cast with these mixes. The content of occluded air may be considered as “normal” (in the order of 3 %).

The main characteristics of a self-compacting hydraulic mixture are mobility, filling ability, and passing ability. Two tests were applied to the IRC and the IIIRC mixes to verify these properties, each of which testing various properties. The slump test was used to evaluate the mobility and the filling ability of the mixes, and the benchmarks for their evaluation were the total spread of the mix and a 500 mm spread-time. The L-box was used to evaluate passing ability and the mobility of the concrete mass. According to the Structural Code [48], IRC achieved an SF2 consistency class and IIIRC achieved an SF1 consistency class, the viscosity (spread of 500 mm) of both mixes was VS2 and the passing ability of both was PL2. In this case, no vibration was required in the casting process of the beams. Both mixes (IRC, IIIRC) showed notably high values (5–7 %) of occluded air, a circumstance that might negatively affect some of their mechanical properties [49,50], especially in the case of IIIRC.

The theoretical densities of the fresh concrete mixes are displayed in the last row of Table 4, and, as foreseen, the mixes with higher quantities of EAFS showed higher densities. Those theoretical values were experimentally verified (see results in Table 5) and the real values were slightly lower, due to notable amounts of occluded air and measurement imprecision.

The evaluation of plastic shrinkage in the drying/setting of fresh mixtures during the first 24 h after mixing and pouring, using an 800-long “gutter tray” coupled to a micrometer, was also notable. As shown in Fig. 3, the first eight hours were the most significant, the values having practically stabilized after 24 h. In the case of the EAFS mixtures, admissible values in reinforced concrete of about 0.5/0.7 mm per meter were found. However, surprisingly larger values were noted in the RCA mixtures, greater than 1.4 mm/m, which

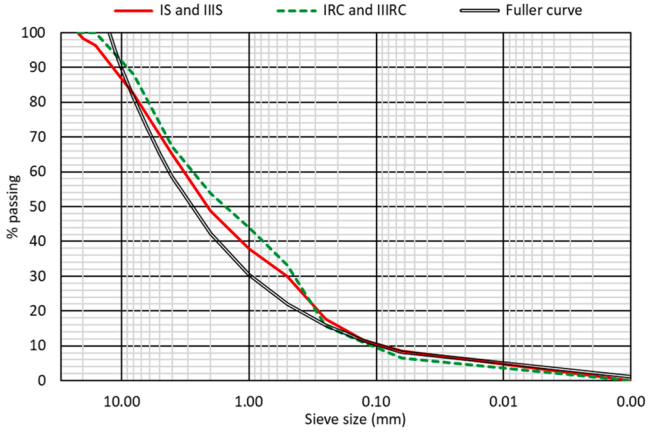

Fig. 2. Granulometry of the mixes in volume and Fuller’s curve.

Table 4
Mix proportions in kg/m^3 of concrete.

	IS and IIIS	IRC and IIIRC
Cement I or Cement III/A	300 (14 % of LFS in IS)	300 (14 % of LFS in IRC)
Water	120	120
EAFS coarse (12–20 mm)	450	-
EAFS medium (4–12 mm)	610	-
EAFS fine (0–4 mm)	660	-
RCA medium (4–12.5 mm)	-	580
RCA fine (0–4 mm)	-	600
Siliceous sand (0–4 mm)	-	300
Limestone fines LFQ (< 0.6 mm)	640	360
Admixtures (% cement weight)	1.3 %	2 %
Total weight (kg per m^3)	2790	2260

Table 5
Fresh mixes properties.

	Consistency Slump/Spreading (t_{500})	Fresh Density (Mg/m^3)	Occluded air (%)	Plastic Shrinkage 12 h (mm)
IS	210/- mm	2.73	3.8	0.65
IIIS	165/- mm	2.75	2.8	0.48
IRC	-/700 mm (4.0 s) L-box 0.9	2.22	4.8	1.42
IIIRC	-/580 mm (4.8 s) L-box 0.8	2.14	6.8	1.64

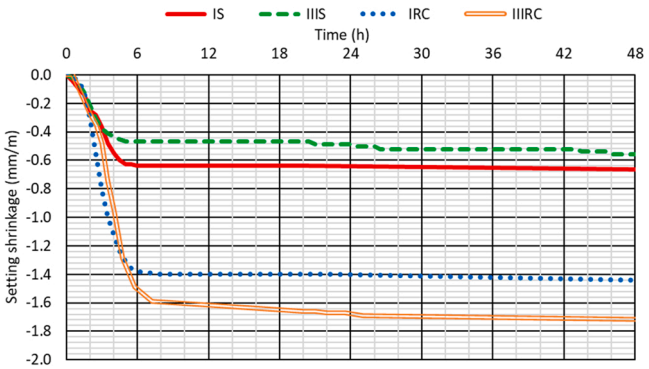

Fig. 3. Short term plastic shrinkage.

pointed to the eventual appearance of plastic shrinkage problems, in the form of cracking, affecting the "*in situ*" construction of structures. Plastic shrinkage is therefore an important practical issue that should be considered in the design and mass production of concretes containing RCA.

5. Physical hardened properties, strength and stiffness

Several properties of the hardened mixtures, measured on samples conserved in a moist chamber at 20ºC and at 98 % relative humidity for over one year, are presented in Table 6.

Furthermore, in this work a set of 100 × 200 mm cylindrical samples of each mixture (6 samples per batch) were poured and placed on the large structural components (beams), up until the tests. Labelled 'companion samples', they were intended to represent the

Table 6
Hardened properties of the mixes conserved in the moist room.

	Hardened dry density (Mg/m^3)	E (GPa) after 28 days in moist room	Coefficient of Poisson	Compression strength after 28–90-180–360 days in moist room (MPa)	Indirect tensile strength (MPa)	Water penetration depth (mm)	
						Maximum	Average
IS	2.71	42	0.22	52–54–55–56	3.75	25.1	20.3
IIIS	2.72	43	0.22	52–56–60–63	4.83	24.0	9.0
IRC	2.21	28	0.19	45–47–50–52	3.45	41.1	24.0
IIIRC	2.1	24	0.18	38–43–48–50	3.35	23.4	16.5

concrete-beam performance in a more realistic way, under the influence of the neighboring environment, rather than within the moist chamber. As can be seen in Table 7, the mechanical properties of the companion samples differed notably from the properties of the samples held in the moist chamber. As the companion samples had been conserved besides the beams in the indoor environment of a test shed, in a dry climate region (in Burgos-Spain, a climatic zone with cold winters and warm summers, and annual mean R.H. of 55 %), their mechanical properties were weaker.

The dry densities shown in the second column of Table 5 were coherent with the fresh densities. The hardened state values were slightly lower, and the difference between the heavier slag aggregate mixtures and the recycled concrete mixtures was approximately 20 %.

The concrete strength of samples after 28, 90, 180, and 360 days in the moist chamber is detailed in Table 6. The strength of all the mixes was suitable for use in structural concretes. Until 28 days, strength could be divided into two batches, one for each aggregate type. The mixtures manufactured with the type-S aggregates reached strengths over and above 50 MPa (which becomes 40 MPa in the companion samples), while mixtures manufactured with the type-RC aggregates were 38–45 MPa (32–38 MPa in the case of the companion samples). The strength levels of the CEM III/A cement mixtures were similar to those obtained using the CEM I cement with a certain proportion of added LFS; a result that reflected the initial intention of the authors of this study.

It is also a remarkable fact that the temporal evolution of compressive strength from 28 to 180 days in the companion samples was observed as an almost constant function, slightly decreasing in the case of the IIIS and the IRC mixtures. That decrease can hardly be considered significant (being almost negligible) with respect to its magnitude, but as a basic concept it was significant, in so far as it pointed to an almost null increase of strength over time in the real beams from the initial 28-day indoor period.

The elastic moduli of the mixtures were measured in cylindrical samples of 100 × 200 mm instrumented with six (3 L and 3 T) strain gauges [51]. Samples containing the type-S aggregate, after 28 days of curing in the moist room, reached 42–43 GPa, with a Poisson ratio of 0.22 units, while the mixtures manufactured with the type-RC aggregates had moduli of 28–24 GPa and a Poisson ratio of 0.18–0.19 units after 28 days, as shown in Table 6. In the case of companion samples, Table 7, lower Young's moduli values were recorded: 38–37 GPa, in the slag aggregate mixtures, and 23–25 GPa in the RCA mixtures. The Poisson ratio values were also slightly lower. Good correlations between the compressive strengths and the elastic moduli of the mixtures are displayed in Fig. 4, depending on the type of aggregate, and based on potential functions. It might be relevant here to recall the formulation $E(MPa) = 4700 \cdot SQRT(f_c)$ that is specified in the ACI code for any concrete [52]. In our case, we have a stiff aggregate (EAFS) with a coefficient of 5850 units and a more compliant aggregate (RCA) with a coefficient of 4110 units.

The water penetration under pressure of the mixes was evaluated in cylindrical samples of 150 × 300 mm, after the specimens had passed 28 days in the moist room and 30 days in an "environmental chamber" (22ºC and 60 % R.H.). This type of specimen was also used in the Brazilian (splitting) test for evaluating the indirect tensile strength of the mixes. In Table 6, mixture permeability to a pressurized flow of water showed a quality range of "medium-permeability" concretes (fairly similar values), with values similar to the conventional maximum threshold of 25 mm and higher than the average of 15 mm. The mixes of better-quality, *i.e.*, lower water penetration, corresponded to the CEM III/A cement, while the CEM I cement mixes yielded more permeable materials, especially IRC. An observation that will be discussed later on.

Likewise, the results of the indirect tensile strength test or Brazilian test pointed to good quality concrete mixes, values also included in Table 6. Again, the better quality of this mechanical property corresponded to mixtures containing EAFS as aggregate.

6. Volume stability: long term shrinkage

The long-term dry shrinkage of the concretes was measured using prismatic specimens of 75×75×285mm in size. These samples had been cured over 28 days underwater and were subsequently stored with the other concrete components for testing in the test shed, simulating the environmental conditions of real concrete structures. The elongation of three specimens of each mix type was evaluated in a rigid frame with a micrometer, and the results represented the average of three measurements. The length variation over almost a year is depicted in Fig. 5a (linear variation) and Fig. 5b (semi-logarithmic scales).

On the one hand, the results of shrinkage values were smaller in the slag-aggregate mixes IIIS, IS (0.7–0.8 mm per meter) than in the RCA mixes (about 0.9–1.1 mm per meter) [53]. On the other hand, the mixes manufactured with the CEM III cement showed lower shrinkage than those manufactured with the CEM I cement. In all, these values were considered acceptable, but slightly high in the field of structural concrete, because the use of conventional natural aggregate in these concrete mixes mainly leads to lower long-term shrinkage values, in the order of 0.5–0.6 thousandths. Another volumetric circumstance that must be taken into account in the design of complex engineering structures.

Logarithms can be successfully used to adjust the data over time on the x axis; see Fig. 5b, in which two regions are clearly distinguishable. In the "first region", a higher slope is shown, which implies a quicker loss of inter-crystalline and/or interlayer water

Table 7
Hardened properties of the companion samples conserved in the test shed.

	E (GPa) at 28 days	Poisson coefficient ν	Compression strength after 28/180 days
IS	37	0.2	42/42
IIIS	38	0.2	42/41
IRC	25	0.18	38/35
IIIRC	23	0.17	32/33

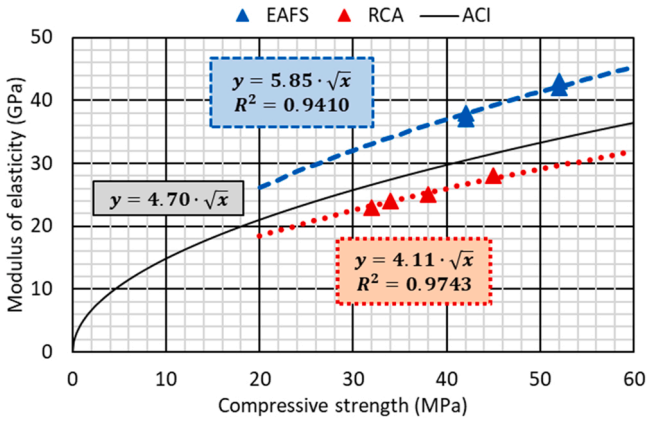

Fig. 4. Correlation compressive strength and stiffness, samples at 28-days in any condition.

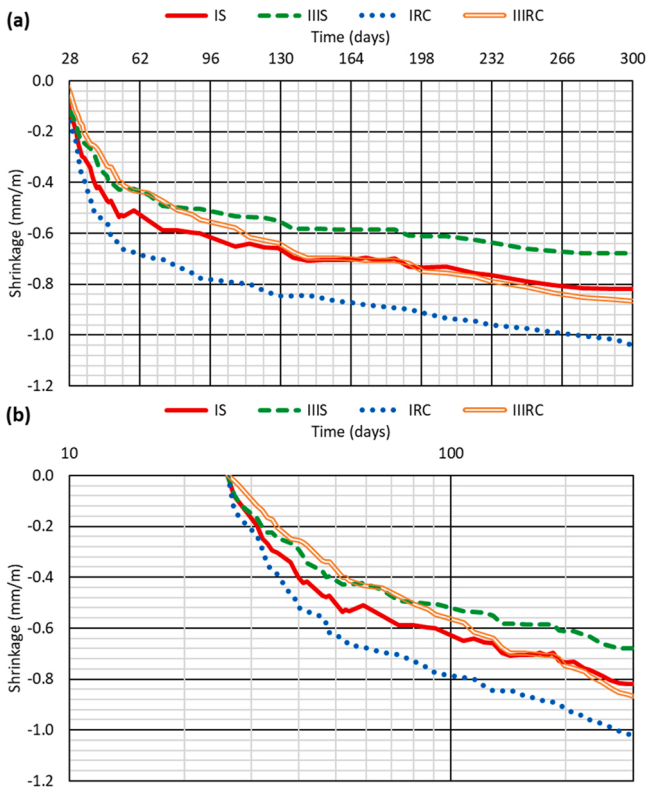

Fig. 5. Shrinkage of concrete mixtures: (a) linear; (b) semi-logarithmic.

that can persist between 28 and 50 days. A "second period" from 50 to 300 days corresponded to a slower rate of water loss. The average slope of the lines in this second period is higher for the RC mixtures (IRC, IIIRC) than for the EAFS-based mixtures (IS, IIIS).

7. Capillary water penetration test. Porosity, Permeability, MIP

Permeability and porosity tests on concrete mixes are commonly developed to look for data on the internal micro-meso-structure and to show correlations between durability, mechanical strength, and microstructure [54,55].

Cubic specimens with 100 mm edges, cured in the moist room for 180 days and subsequently "conditioned", were used to evaluate the capillarity water absorption of the mixes, following the specifications of the ASTM C-1585 standard "Measurement of ratio of absorption of water by hydraulic cement concretes" [56], also known as the "Fagerlund method". The test reveals the suction capacity of a hardened concrete as water rises by capillary action from the bottom to the top. The objective of the test, which quantifies the

water permeation in porous media based on the Darcy's laws, is to evaluate the porosity, connectivity and hydrophilicity of the mix, to gain an idea of the global quality of the mixes.

The results are displayed in the three left-hand columns of Table 8, using the units (m, g, min) of the Darcy permeation tests. A scratched lower face of the sample is placed on a fine gravel course laid on the bottom of a tray with 1 cm of water. The gain of mass of the sample is measured and plotted against the square root of time, as shown in Fig. 6. The test ends when no further mass is gained, which means that the specimen is saturated, and that water absorption has stabilized.

In Table 8, the column headings ε_e and k refer to effective porosity the capillary absorption coefficient, respectively. The values for these magnitudes indicated that the test mixes were, in general, of acceptable quality. In fact, effective porosity values of approximately 12 % can be qualified as good and values of 15 % as common; mixtures made with EAFS (12.4–13.6 %) are clearly better than those made using RCA (16 %), which is to be expected according to the literature.

In contrast, regarding the capillary absorption rates (k coefficient, slope within the first region of curves), it is accepted that values below 60 $g/m^2 \cdot min^{0.5}$ denote very good quality concrete. In our case, the CEM III mixtures were of fairly good quality with 82–90 $g/m^2 \cdot min^{0.5}$, while the CEM I mixtures with 116–128 units were tolerable; values over 200 units could be considered indicative of poor-quality mixtures, overly susceptible to the entry of harmful substances.

Water absorption tests through the skin of the samples were performed on cubic 100 mm specimens of all the mixtures, according to standard ASTM C-642 [56]. The first test consisted of measuring the increased weight of the samples over four weeks that had been immersed in water at room temperature. The second test consisted of measuring the increase in sample weight over four weeks totally immersed in boiling water at a constant temperature of 100ºC.

In the first case, immersion at room temperature is used to measure the permeability of the concrete skin, formed by the cementitious matrix of the mixture, after the initial plastic shrinkage mentioned in Section 3. The results are detailed in the fourth column of Table 8 and showed a qualitative coherence with the results on water penetration under pressure in Table 6, showing better results for the mixtures made with CEM III/A cement than the CEM I mixtures.

In the second case, immersion in boiling water was at a temperature above the decomposition temperature of primary ettringite. The characteristics of permeation through the external skin of the samples were altered, and the internal concrete was even damaged to a degree. The amounts of absorbed water are depicted in the fifth column of Table 8; it can be observed that the CEM III/A cement samples showed less increase or even a decrease in absorbed water, while the CEM I cement samples showed an increase. Undoubtedly, primary ettringite is much more abundant in the CEM I cement samples, and its decomposition affected the amount of absorbed water in a more notable way.

Mercury Intrusion Porosimetry (MIP) tests were also performed on small specimens of the mixtures (mass about 3 g) that were extracted from the cementitious matrix, avoiding the presence of visible aggregate fragments. The results are displayed in % MIP porosity, in the sixth column of Table 8. In the graphics of Fig. 7, we have the cumulative intrusion and log differential intrusion values beginning with a 7 nm pore size. Once again, the EAFS mixes had lower values than the corresponding RCA mixes.

According to Metha and Monteiro [57], micro-pore sizes (peaks in Fig. 7b) smaller than 60–70 nm are in practical terms almost inefficient against permeability and mechanical properties. In our mixtures with the CEM III cement, mixes IIIS and IIIRC showed good results (a low slope) in the k-permeability results, which could be clearly associated with the easy transport of water through a fraction of their porosity. In the cumulative intrusion curves to the left of Fig. 7, only 42 % of total porosity (comparing ordinates in abscissa 65 nm and in abscissa 7 nm) was efficient with regard to water intrusion in the IIIRC samples, while in the case of the IIIS samples, this result was 70%. Hence, the efficient porosities were respectively 9.3 % (58 % of 16 %) for IIIRC and 8.7 % (70 % of 12.4 %) for IIIS. Additionally, the peak in 0.55 μm of IIIRC (in log diff. intrusion curve) slightly accelerated the permeation with respect to IIIS; however, the high peak at 60 nm for IIIRC resulted in a longer saturation time (300^2 minutes, 62.5 days) than IIIS, whose saturation time was 275^2 minutes, equivalent to 52.5 days. In fact, the results of capillary absorption and MIP were largely coherent.

In the same way, a similar analysis of the CEM I cement, mixtures IRC and IS, yielded porosities of 11.8 % (75 % of 15.8 %) in IRC, and 10.9 % (80 % of 13.6 %) in IS, which were to some extent detrimental. Additionally, the higher peak in 0.12 μm of IRC (in log diff. intrusion curve) slightly slowed down the permeation with regard to IS. In all, the permeability indexes of cement I mixtures were higher than the type III cement mixtures, as shown in Table 8, a factor which can be eventually reflected in the durability results.

8. Chloride ion penetration

Standard EN 12390-11 [41] offers guidance on the experimental procedure of a chlorine penetration test. Cubic samples of 100 mm, saturated in drinking water, were submerged and lay on their lower faces at a depth of 10 mm in a solution of 3.5 % of marine salt. Chlorine ions absorbed by capillary action and diffusion from the bottom towards the upper zone of the samples placed in water over 36 days produced the concentration profiles shown in Fig. 8.

Table 8
Capillary test results.

	ε_e (%)	k ($g/m^2 \cdot min^{0.5}$)	Absorption (g)	Boiling absorption (g)	MIP porosity (%)	Efficient porosity (%)	Chlorine diffusion D (m^2/s)
IS	13.6	128	43.6	46	11.5	10.9	$1.7 \cdot 10^{-10}$
IIIS	12.4	82	26.1	28	14.7	8.7	$8.8 \cdot 10^{-11}$
IRC	15.8	116	52.6	60	14.5	11.8	$1.6 \cdot 10^{-10}$
IIIRC	16	90	47.1	35	20.3	9.3	$7.6 \cdot 10^{-11}$

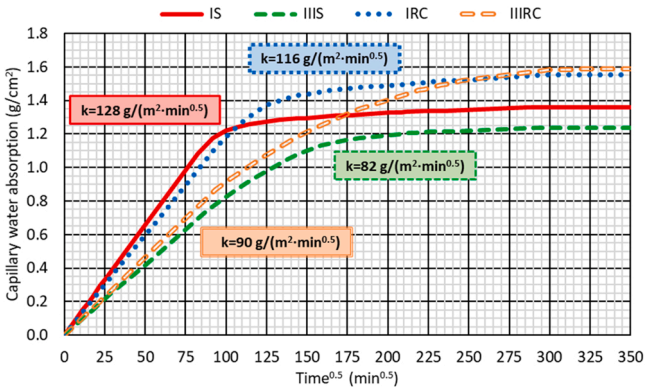

Fig. 6. Capillary water absorption in mass per unit area.

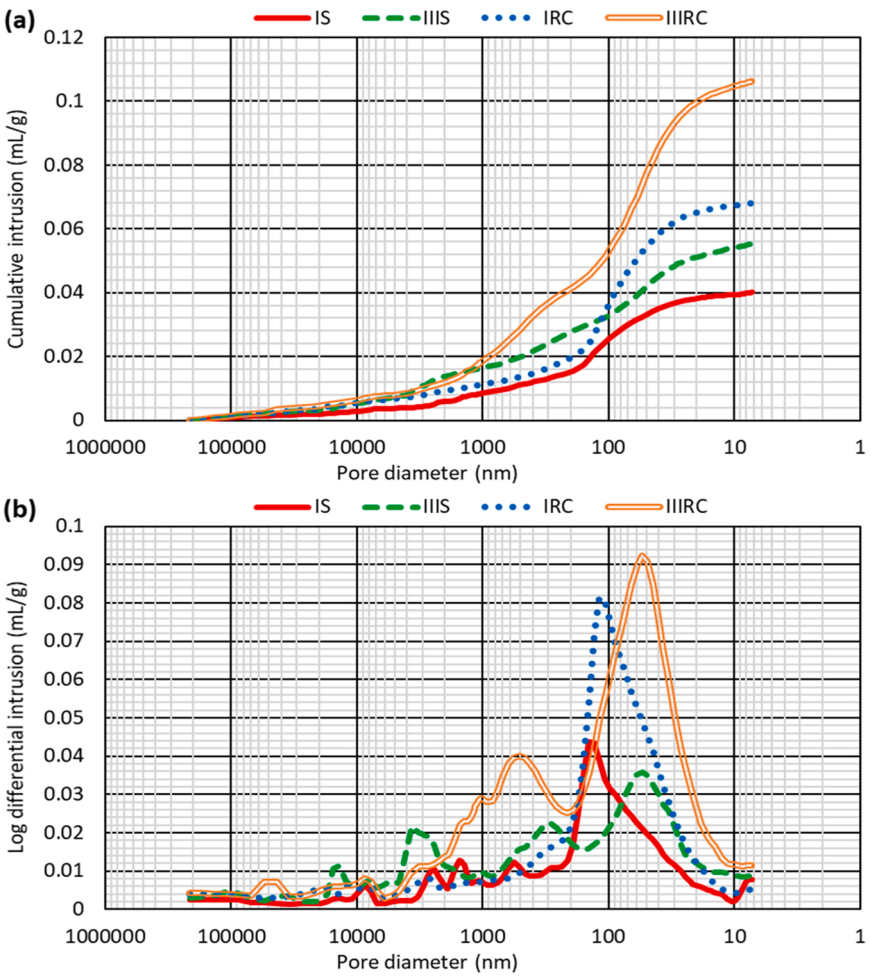

Fig. 7. MIP porosity results: (a) cumulative intrusion; (b) log differential intrusion.

Chloride ion penetration in the mass of concrete is a direct function of its capillary permeability to water (chlorides are water soluble), moderated by partial ion-fixation on the substances that compose the material. A global mathematical approximation of steady-state chloride diffusion is usually estimated through the solution to the error function of Fick's second law of diffusion applied to transient diffusion. It yields an estimate of an apparent diffusion coefficient for each different mixture after the analysis of the test results on a set of concrete mixes. Several values are proposed for the apparent diffusion coefficient, D, in the far right-hand-side

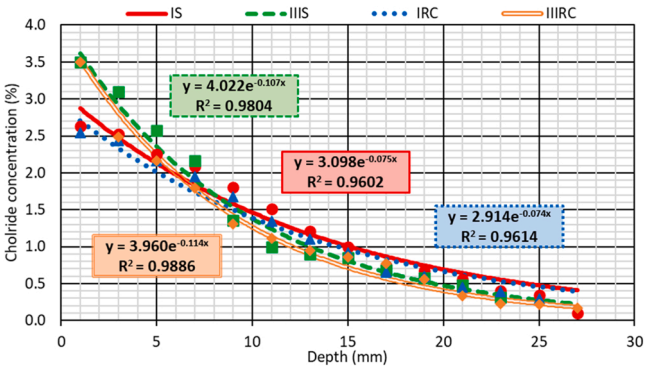

Fig. 8. Interpolations in the chlorine ion penetration profiles.

column of Table 8.

The results of chloride ion concentrations, measured with EDX-SEM on samples of the different mixtures are depicted in Fig. 8. One such example is shown in Fig. 9. Exponential regressions are shown in Fig. 8 to manage the natural scatter of the experimental results and to determine the penetration data type which yields the numerical values of the diffusion coefficient, D. In fact, the authors obtained this value based on data values of deep penetration (variable x in the second of Fick's law on diffusion, a monomial expression, $x / 2\sqrt{Dt}$) in which the chlorine concentration was 1 %. The values obtained for chlorine diffusivity in these mixtures were within an acceptable order of magnitude.

The superficial concentrations of chloride ion adsorbed on the entry surface of the samples differed between the two groups of mixes. Mixtures based on CEM III/A showed superficial concentrations of around 4 %, while the CEM I mixes showed around 3 %, as may be seen in the equations in Fig. 8; all these values are certainly high and not too reassuring. Some similar results were found by the authors in earlier works, in which the samples were submerged for over one year in sea water. In 2018, Santamaria et al. obtained better results for self-compacting slag mixes [58] that showed surface Cl concentrations of 0.5 % in most of mixes and 2.2 % in the worst case; later on, in 2021, Sosa et al. [59] obtained similar and lower results (1.2 % and 2 % Cl in the surface) for penetration in well performed slag mixtures when researching applications for use in marine environments.

Despite the above-mentioned circumstance, the penetration rate in the CEM III/A cement mixes was slower than in the CEM I mixes, reaching 1 % of chlorine concentration at depths of 12 mm (IIIRC) and 13 mm (III/S), while the concentrations in the CEM I mixes reached around 1 % at depths of 14.5- and 15-mm. The difference was not enormous, although as has been well known for many years, the CEM III/A cement presents advantages for use in marine water, as confirmed by the MIP test results in the preceding section. However, the influence of the type of aggregate (slag, RCA) is of minor importance, though slightly more favorable advantages of RCA have been found in this research.

9. Conclusions

Following the experimental work developed in this research, several conclusions useful for additions of slag and recycled concrete aggregate in mixtures of structural concrete can be advanced.

Firstly, the authors have noted that the differences between the results of the standardized laboratory tests on moist room conserved samples, and the tests on the real concrete cured in the workplaces conditions, were notable; the compressive strength after 90 days fell by a factor of 0.7 units; in the S-mixes from 60 to 42 MPa, and in the RCA mixes from 51 to 35 MPa in average.

Secondly, excellent sustainable structural concrete mixtures may be performed using a reduced proportion of Portland clinker, in the order of 230–150 kg per cubic meter of concrete, including suitable SCM and minimizing the carbon footprint of the production

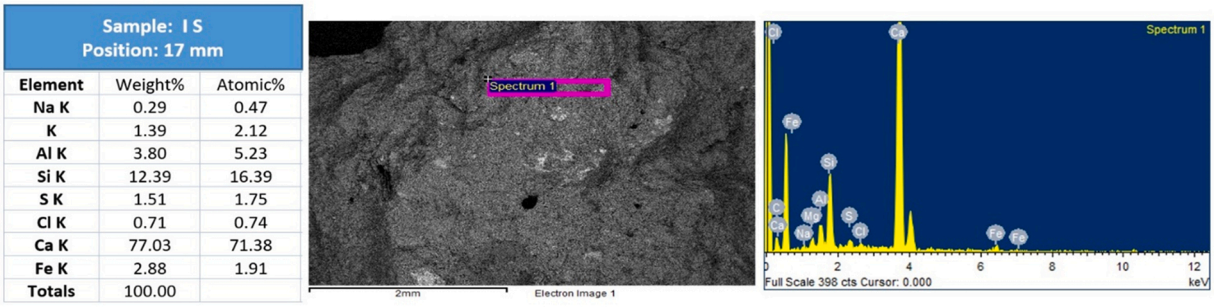

Fig. 9. Examples of EDX-SEM results.

runs.

Suitable proportioning, a key question in the efficient preparation of this sort of concrete, is recommended. Accordingly, the inclusion of a siliceous river sand fraction, sized 0–4 mm weighing 300 kg per cubic meter, was decisive for enhancing the global properties of the RCA mixtures.

Both sorts of mixtures, containing EAFS and RCA, showed notable variability in their fresh and hardened densities, from 2.7 to 2.2 Mg/m^3; furthermore, their workability was in all cases acceptable for use in structural construction. An important point to mention was the high level of plastic shrinkage over, 1.2 thousandth, during the setting of the RCA mixes.

With regard to the permeability of the CEM III/A mixtures, the advantages against chemical attack were evident, due to the fineness of their capillary networks, which adds weight to their application in civil and structural engineering; the use of the CEM I-based mixtures was undoubtedly admissible.

The chloride penetration rates were relatively high in all the mixtures under analysis, showing a value of 3/3.5 % of chlorine adhered to the surface of the samples submerged in the standardized saline solution. This circumstance constituted a negative feature in relation to steel slag reinforcement protection in marine environments and roadways in winter weather.

CRediT authorship contribution statement

Amaia Santamaría: Conceptualization, Methodology, Investigation, Data curation, Software Writing – original draft. **Víctor Revilla-Cuesta:** Conceptualization, Methodology, Investigation, Data curation, Software, Writing – original draft. **Marta Skaf:** Investigation, Data curation, Supervision, Writing – review & editing, Resources, Funding acquisition. **Jesús M. Romera:** Investigation, Data curation, Supervision, Writing – review & editing, Resources, Funding acquisition.

Declaration of Competing Interest

The authors declare that they have no known competing financial interests or personal relationships that could have appeared to influence the work reported in this paper.

Data availability

Data will be made available on request.

Acknowledgements

The authors wish to express their gratitude to the following entities for the funding they provided: MCIN/AEI/10.13039/501100011033 and ERDF A way of making Europe, the European Union, and Next Generation EU/PRTR [PID2020-113837RB-I00; PID2021–124203OB-I00 and TED2021-129715B-I00]; the Junta de Castilla y León (Regional Government) and ERDF [UIC-231]; the Basque Government [IT1619-22 SAREN Research Group]; the University of Burgos [Y135. GI].

References

[1] R.H. Faraj, H.U. Ahmed, S. Rafiq, N.H. Sor, D.F. Ibrahim, S.M.A. Qaidi, Performance of self-compacting mortars modified with nanoparticles: a systematic review and modeling, Clean. Mater. 4 (2022), 100086, https://doi.org/10.1016/j.clema.2022.100086.

[2] S.N. Ahmed, N. Hamah Sor, M.A. Ahmed, S.M.A. Qaidi, Thermal conductivity and hardened behavior of eco-friendly concrete incorporating waste polypropylene as fine aggregate, Mater. Today Proc. 57 (2022) 818–823, https://doi.org/10.1016/j.matpr.2022.02.417.

[3] V. Malhotra, in: Proceedings of the SP-202: Third Canmet/ACI International Symposium: Sustainable Development of Cement and Concrete, ACI Special Publication (2001).

[4] F. Faleschini, P. De Marzi, C. Pellegrino, Recycled concrete containing EAF slag: Environmental assessment through LCA, Eur. J. Environ. Civ. Eng. 18 (9) (2014) 1009–1024, https://doi.org/10.1080/19648189.2014.922505.

[5] C. Pellegrino, F. Faleschini, Sustainability improvements in the concrete industry: use of recycled materials for structural concrete production. Green Energy and Technology Series, Springer, 2016, https://doi.org/10.1007/978-3-319-28540-5.

[6] A. Neves, J. Almeida, F. Cruz, T. Miranda, V.M.C.F. Cunha, M. Rodrigues, J. Costa, E.B. Pereira, Design procedures for sustainable structural concretes using wastes and industrial by-products, Appl. Sci. 13 (4) (2023) 2087, https://doi.org/10.3390/app13042087.

[7] H. Qasrawi, The use of steel slag aggregate to enhance the mechanical properties of recycled aggregate concrete and retain the environment, Constr. Build. Mater. 54 (2014) 298–304, https://doi.org/10.1016/j.conbuildmat.2013.12.063.

[8] M.M. Al-Tayeb, Y.I.A. Aisheh, S.M.A. Qaidi, B.A. Tayeh, Experimental and simulation study on the impact resistance of concrete to replace high amounts of fine aggregate with plastic waste, Case Stud. Constr. Mater. 17 (2022), e01324, https://doi.org/10.1016/j.cscm.2022.e01324.

[9] A. Ebrahim Abu El-Maaty Behiry, Utilization of cement treated recycled concrete aggregates as base or subbase layer in Egypt, Ain Shams Eng. J. 4 (4) (2013) 661–673, https://doi.org/10.1016/j.asej.2013.02.005.

[10] L. Evangelista, J.De Brito, Concrete with fine recycled aggregates: a review, Eur. J. Environ. Civ. Eng. 18 (2) (2014) 129–172, https://doi.org/10.1080/19648189.2013.851038.

[11] V. Revilla-Cuesta, V. Ortega-López, M. Skaf, J.M. Manso, Effect of fine recycled concrete aggregate on the mechanical behavior of self-compacting concrete, Constr. Build. Mater. 263 (2020), 120671, https://doi.org/10.1016/j.conbuildmat.2020.120671.

[12] R.V. Silva, J. De Brito, R.K. Dhir, The influence of the use of recycled aggregates on the compressive strength of concrete: a review, Eur. J. Environ. Civ. Eng. 19 (7) (2015) 825–849, https://doi.org/10.1080/19648189.2014.974831.

[13] F. Fiol, C. Thomas, C. Muñoz, V. Ortega-López, J.M. Manso, The influence of recycled aggregates from precast elements on the mechanical properties of structural self-compacting concrete, Constr. Build. Mater. 182 (2018) 309–323, https://doi.org/10.1016/j.conbuildmat.2018.06.132.

[14] M. Skaf, V. Ortega-López, J.A. Fuente-Alonso, A. Santamaría, J.M. Manso, Ladle furnace slag in asphalt mixes, Constr. Build. Mater. 122 (2016) 488–495, https://doi.org/10.1016/j.conbuildmat.2016.06.085.

[15] I.Z. Yildirim, M. Prezzi, Use of Steel Slag in Subgrade Applications, Publication FWA/IN/JTRP-2009/32, Joint Transportation Research Program, Indiana Department of Transportation and Purdue University, West Lafayette, Indiana (2009).
[16] P. Bosela, N. Delatte, R. Obratil, A. Patel, Fresh and hardened properties of paving concrete with steel slag aggregate, Carreteras 4 (166) (2009) 55–66.
[17] B. Fronek, P. Bosela, N. Delatte, Steel slag aggregate used in portland cement concrete, Transp. Res. Rec. (2012) 37–42, https://doi.org/10.3141/2267-04.
[18] A.M. Rashad, Behavior of steel slag aggregate in mortar and concrete - a comprehensive overview, J. Build. Eng. 53 (2022), 104536, https://doi.org/10.1016/j.jobe.2022.104536.
[19] A.S. Brand, E.O. Fanijo, A review of the influence of steel furnace slag type on the properties of cementitious composites, Appl. Sci. 10 (22) (2020) 1–27, https://doi.org/10.3390/app10228210.
[20] V. Ortega-López, J.A. Fuente-Alonso, M. Skaf, A. Santamaría, A. Aragón, J.M. Manso, Performance of steel-making slag concrete reinforced with fibers, MATEC Web Conf. 120 (2017) 04001, https://doi.org/10.1051/matecconf/201712004001.
[21] F. Özalp, Effects of electric arc furnace (EAF) slags on mechanical and permeability properties of paving stone, kerb and concrete pipes, Constr. Build. Mater. 329 (2022), 127159, https://doi.org/10.1016/j.conbuildmat.2022.127159.
[22] B.S. Cho, Y.C. Choi, Hydration properties of STS-refining slag-blended blast furnace slag cement, Adv. Mater. Sci. Eng. 2018 (2018), 5893254, https://doi.org/10.1155/2018/5893254.
[23] S.I. Abu-Eishah, A.S. El-Dieb, M.S. Bedir, Performance of concrete mixtures made with electric arc furnace (EAF) steel slag aggregate produced in the Arabian Gulf region, Constr. Build. Mater. 34 (2012) 249–256, https://doi.org/10.1016/j.conbuildmat.2012.02.012.
[24] J.M. Manso, D. Hernández, M.M. Losáñez, J.J. González, Design and elaboration of concrete mixtures using steelmaking slags, Acids Mater. J. 108 (6) (2011) 673–681.
[25] S. Monosi, M.L. Ruello, D. Sani, Electric arc furnace slag as natural aggregate replacement in concrete production, Cem. Concr. Compos. 66 (2016) 66–72, https://doi.org/10.1016/j.cemconcomp.2015.10.004.
[26] M. Pasetto, N. Baldo, Experimental evaluation of high performance base course and road base asphalt concrete with electric arc furnace steel slags, J. Hazard. Mater. 181 (1–3) (2010) 938–948, https://doi.org/10.1016/j.jhazmat.2010.05.104.
[27] M. Pasetto, N. Baldo, Mix design and performance analysis of asphalt concretes with electric arc furnace slag, Constr. Build. Mater. 25 (8) (2011) 3458–3468, https://doi.org/10.1016/j.conbuildmat.2011.03.037.
[28] M. Skaf, J.M. Manso, Á. Aragón, J.A. Fuente-Alonso, V. Ortega-López, EAF slag in asphalt mixes: a brief review of its possible re-use, Resour. Conserv. Recycl. 120 (2017) 176–185, https://doi.org/10.1016/j.resconrec.2016.12.009.
[29] B.S. Cho, Y.C. Choi, Properties of cementless binders using desulfurization slag as an alkali activator, J. Ceram. Process. Res 19 (1) (2018) 37–42.
[30] J.M. Montenegro-Cooper, M. Celemín-Matachana, J. Cañizal, J.J. González, Study of the expansive behavior of ladle furnace slag and its mixture with low quality natural soils, Constr. Build. Mater. 203 (2019) 201–209, https://doi.org/10.1016/j.conbuildmat.2019.01.040.
[31] S. Qaidi, Y.S.S. Al-Kamaki, R. Al-Mahaidi, A.S. Mohammed, H.U. Ahmed, O. Zaid, F. Althoey, J. Ahmad, H.F. Isleem, I. Bennetts, Investigation of the effectiveness of CFRP strengthening of concrete made with recycled waste PET fine plastic aggregate, PLoS ONE 17 (2022), e0269664, https://doi.org/10.1371/journal.pone.0269664.
[32] S.M.A. Qaidi, B.A. Tayeh, A.M. Zeyad, A.R.G. de Azevedo, H.U. Ahmed, W. Emad, Recycling of mine tailings for the geopolymers production: a systematic review, Case Stud. Constr. Mater. 16 (2022), e00933, https://doi.org/10.1016/j.cscm.2022.e00933.
[33] F. Faleschini, M. Alejandro Fernández-Ruíz, M.A. Zanini, K. Brunelli, C. Pellegrino, E. Hernández-Montes, High performance concrete with electric arc furnace slag as aggregate: mechanical and durability properties, Constr. Build. Mater. 101 (2015) 113–121, https://doi.org/10.1016/j.conbuildmat.2015.10.022.
[34] C. Pellegrino, P. Cavagnis, F. Faleschini, K. Brunelli, Properties of concretes with black/oxidizing electric arc furnace slag aggregate, Cem. Concr. Compos. 37 (1) (2013) 232–240, https://doi.org/10.1016/j.cemconcomp.2012.09.001.
[35] A. Santamaría, A. Orbe, M.M. Losañez, M. Skaf, V. Ortega-Lopez, J.J. González, Self-compacting concrete incorporating electric arc-furnace steelmaking slag as aggregate, Mater. Des. 115 (2017) 179–193, https://doi.org/10.1016/j.matdes.2016.11.048.
[36] I. Marcos, J.T. San-José, L. Garmendia, A. Santamaría, J.M. Manso, Central lessons from the historical analysis of 24 reinforced-concrete structures in northern Spain, J. Cult. Herit. 20 (2016) 649–659, https://doi.org/10.1016/j.culher.2016.03.003.
[37] F. Faleschini, M.A. Zanini, C. Pellegrino, New perspectives in the use of electric arc furnace slag as coarse aggregate for structural concrete, in: Proceedings of the International Conference Euroslag, Linz, Austria, 2015 (2015).
[38] H. Qasrawi, Towards sustainable self-compacting concrete: effect of recycled slag coarse aggregate on the fresh properties of SCC, Adv. Civ. Eng. 2018 (2018) 7450943, https://doi.org/10.1155/2018/7450943.
[39] H. Qasrawi, Fresh properties of green SCC made with recycled steel slag coarse aggregate under normal and hot weather, J. Clean. Prod. 204 (2018) 980–991, https://doi.org/10.1016/j.jclepro.2018.09.075.
[40] J.T. San-José, J.M. Manso, Fiber-reinforced polymer bars embedded in a resin concrete: study of both materials and their bond behavior, Polym. Compos. 27 (3) (2006) 315–322, https://doi.org/10.1002/pc.20188.
[41] CEN, European Committee for Standardization, Rue de Stassart, 36. Brussels B-1050.
[42] H.B. Tran, Mechanical properties of coarse aggregate electric arc furnace slag in cement concrete, Civ. Eng. J. 7 (10) (2021) 1716–1730, https://doi.org/10.28991/cej-2021-03091755.
[43] I.Z. Yildirim, M. Prezzi, Chemical, mineralogical, and morphological properties of steel slag, Adv. Civ. Eng. 2011 (2011), 463638, https://doi.org/10.1155/2011/463638.
[44] C.S.G. Penteado, B.L. Evangelista, G.Cd Ferreira, P.H.A. Borges, R.C.C. Lintz, Use of electric arc furnace slag for producing concrete paving blocks, Ambient. Constr. 19 (2) (2019) 21–32, https://doi.org/10.1590/s1678-86212019000200305.
[45] A. Chatzopoulos, K.K. Sideris, C. Tassos, Production of concretes using slag aggregates: contribution of increasing the durability and sustainability of constructions, Case Stud. Constr. Mater. 15 (2021), e00711, https://doi.org/10.1016/j.cscm.2021.e00711.
[46] S. Zhuang, Q. Wang, T. Luo, Effect of C12A7 in steel slag on the early-age hydration of cement, Cem. Concr. Res. 162 (2022), 107010, https://doi.org/10.1016/j.cemconres.2022.107010.
[47] V. García-Cortés, D. García Estévez, J.T. San-José, Assessment of particle packing models for aggregate dosage design in limestone and EAFS aggregate-based concretes, Constr. Build. Mater. 328 (2022), 126977, https://doi.org/10.1016/j.conbuildmat.2022.126977.
[48] FIB. CEB-FIP, Model Code 2010, Lausanne-Switzerland (2010).
[49] V. Revilla-Cuesta, M. Skaf, F. Faleschini, J.M. Manso, V. Ortega-López, Self-compacting concrete manufactured with recycled concrete aggregate: an overview, J. Clean. Prod. 262 (2020), 121362, https://doi.org/10.1016/j.jclepro.2020.121362.
[50] R.V. Silva, J. de Brito, R.K. Dhir, Fresh-state performance of recycled aggregate concrete: a review, Constr. Build. Mater. 178 (2018) 19–31, https://doi.org/10.1016/j.conbuildmat.2018.05.149.
[51] V. Revilla-Cuesta, M. Skaf, A. Santamaría, J.M. Romera, V. Ortega-López, Elastic stiffness estimation of aggregate–ITZ system of concrete through matrix porosity and volumetric considerations: explanation and exemplification, Arch. Civ. Mech. Eng. 22 (2) (2022) 59, https://doi.org/10.1007/s43452-022-00382-z.
[52] ACI Committees 318M-14 and RM-14, Building Code Requirements for Structural Concrete, American Concrete Institute, Farmington Hills, MI.
[53] A. Gonzalez-Corominas, M. Etxeberria, Effects of using recycled concrete aggregates on the shrinkage of high performance concrete, Constr. Build. Mater. 115 (2016) 32–41, https://doi.org/10.1016/j.conbuildmat.2016.04.031.
[54] M.A. González-Ortega, S.H.P. Cavalaro, G. Rodríguez de Sensale, A. Aguado, Durability of concrete with electric arc furnace slag aggregate, Constr. Build. Mater. 217 (2019) 543–556, https://doi.org/10.1016/j.conbuildmat.2019.05.082.
[55] V. Ortega-López, J.A. Fuente-Alonso, A. Santamaría, J.T. San-José, Á. Aragón, Durability studies on fiber-reinforced EAF slag concrete for pavements, Constr. Build. Mater. 163 (2018) 471–481, https://doi.org/10.1016/j.conbuildmat.2017.12.121.
[56] ASTM, Annual Book of ASTM Standars, ASTM International, West Conshohocken, PA, USA , (2008) 19429-2959.

[57] P.K. Metha, P.J.M. Monteiro. Concrete; Microstructure, Properties and Materials, fourth ed., McGraw-Hill Education, 2014. ISBN 978-0-07-179787-0 (2014).
[58] A. Santamaría, A. Orbe, J.T. San José, J.J. González, A study on the durability of structural concrete incorporating electric steelmaking slags, Constr. Build. Mater. 161 (2018) 94–111, https://doi.org/10.1016/j.conbuildmat.2017.11.121.
[59] I. Sosa, P. Tamayo, J.A. Sainz-Aja, C. Thomas, J. Setien, J.A. Polanco, Durability aspects in self compacting siderurgical aggregate concrete, J. Build. Eng. 39 (2021), 102268, https://doi.org/10.1016/j.jobe.2021.102268.